Redox Biology 86 (2025) 103842

Contents lists available at ScienceDirect

Redox Biology

journal homepage: www.elsevier.com/locate/redox

Strand-specific quantification of 8-oxo-dG and apurinic sites via Ligation-Dependent Probe Amplification (LPA)

Antonella Romano [a,1], Antonia Feola [a,1], Valentina Morgera [a,1], Alfonso Tramontano [b], Samantha Messina [c], Daniel Gackowski [d], Ewelina Zarakowska [d], Ryszard Olinski [d], Vittorio Enrico Avvedimento [b], Candida Zuchegna [e,*], Antonio Porcellini [a,**], Antonio Pezone [a,***]

[a] Department of Biology, Federico II University, 80126, Napoli, Italy
[b] Department of Molecular Medicine and Medical Biotechnology, Federico II University, 80131, Napoli, Italy
[c] Department of Science, Roma Tre University, Viale Guglielmo Marconi 446, 00146, Rome, Italy
[d] Department of Clinical Biochemistry, Faculty of Pharmacy, Collegium Medicum in Bydgoszcz, Nicolaus Copernicus University in Toruń, 85-095, Bydgoszcz, Poland
[e] Department of Epidemiology, Preclinical Research and Advanced Diagnostics, National Institute for Infectious Diseases IRCCS L. Spallanzani, Rome, Italy

ARTICLE INFO

Keywords:
DNA oxidation
Strand-specific DNA damage
8-oxo-dG
Apurinic sites
DNA repair
Ligation-dependent probe amplification

ABSTRACT

Oxidative DNA damage, characterized by the prominent lesion 8-oxo-7,8-dihydroguanine (8-oxo-dG), is linked to mutagenesis and genome instability. Accurately mapping these lesions with strand specificity and high resolution remains a major challenge, limiting our understanding of damage dynamics during transcription and repair. Here, we introduce a novel, highly sensitive ligation-dependent probe amplification (LPA) method that enables quantitative, strand-specific analysis of 8-oxo-dG and apurinic (AP) sites at single-nucleotide resolution. Our technique uses enzymatic digestion, highly selective ligation, and quantitative PCR to distinguish damaged from intact DNA strands, offering detailed insight into lesion localization and repair kinetics. When applied to estrogen-stimulated breast cancer cells, LPA reveals asymmetric, strand-specific guanine oxidation during transcriptional activation, characterized by rapid repair of the transcribed strand and more persistent damage on the non-transcribed strand. Our findings show that oxidative lesions are dynamically regulated by biological stimuli, reflecting a finely tuned balance between repair and damage buildup. This LPA approach is a powerful tool for exploring the complex relationship among redox signaling, DNA damage, and transcription regulation, furthering our understanding of redox-driven genome modulation in health and disease.

1. Introduction

Oxidative DNA damage, particularly the formation of 8-oxo-7,8-dihydroguanine (8-oxo-dG), poses a significant threat to genome integrity. As a common and mutagenic oxidative lesion, 8-oxo-dG leads to point mutations, genomic instability, and disease development by disrupting cellular homeostasis [1]. Beyond its mutagenic effects, 8-oxo-dG influences the structural and regulatory aspects of DNA by decreasing helical stability and interfering with transcriptional accuracy through its interactions with DNA repair intermediates [2]. Additionally, 8-oxo-dG serves as a platform for recruiting key repair enzymes such as 8-oxo-dG glycosylase (OGG1) and apurinic/apyrimidinic endonuclease 1 (APE1). These enzymes coordinate the repair of oxidative damage while interacting with the transcriptional machinery [3].

Recent studies indicate that 8-oxo-dG functions as an epigenetic marker associated with transcriptional activation, signaling gene regulation events [4]. This has been observed during hormone-triggered transcription responses across various biological systems [5,6]. Activation of transcription following exposure to estrogen or retinoic acid involves lysine-specific demethylases such as KDM1 and 2-oxoglutarate (2OG)-dependent dioxygenases. These enzymes catalyze histone demethylation, producing hydrogen peroxide (H_2O_2) as a byproduct. When

* Corresponding author.
** Corresponding author.
*** Corresponding author.
E-mail addresses: candida.zuchegna@inmi.it (C. Zuchegna), antonio.porcellini@unina.it (A. Porcellini), antonio.pezone@unina.it (A. Porcellini).
[1] equally contributed.

https://doi.org/10.1016/j.redox.2025.103842
Received 13 August 2025; Accepted 22 August 2025
Available online 23 August 2025

transition metals, particularly ferrous ions (Fe^{2+}), are present, H_2O_2 undergoes the Fenton reaction, generating hydroxyl radicals (·OH) that cause site-specific oxidative DNA damage [7].

Additionally, the Haber-Weiss reaction regenerates Fe^{2+} by reducing Fe^{3+} with superoxide (O_2^-), which then enters the Fenton cycle. Both reactions produce localized ·OH, which oxidizes guanine to 8-oxo-dG and alters DNA structure in transcriptionally active regions [8]. OGG1 is subsequently recruited to remove 8-oxo-dG, creating apurinic sites. APE1 then cleaves the phosphodiester backbone at these sites, enabling the assembly of the topoisomerase IIβ (TOPIIβ) complex, essential for transcription initiation. Importantly, this sequence extends beyond nuclear receptor-mediated gene activation to include broader transcriptional regulators such as TGFβ and c-Myc [9,10].

Currently, liquid chromatography-tandem mass spectrometry (LC-MS/MS) is the gold standard for measuring DNA oxidation because of its high sensitivity and specificity. However, many techniques depend on indirect detection or fluorescent labeling of 8-oxo-dG, which may introduce methodological biases. While gas chromatography-mass spectrometry (GC-MS) provides accurate quantification, its multistep derivatization procedures often cause artifactual guanine oxidation, especially during DNA hydrolysis or heat treatment [11,12]. ELISA and immunofluorescence, though accessible and sensitive, may not be able to differentiate among various oxidative lesions or offer enough resolution for detailed mapping [13,14].

The comet assay, commonly used to evaluate overall DNA damage, has a variant modified with FpG designed to detect oxidative base damage. However, this method faces reproducibility issues and lacks single-nucleotide resolution [15,16]. In recent years, high-throughput sequencing-based techniques, such as AP-seq [17], Click-code-seq [18], and Nanopore technologies [19], have been used to map the distribution of 8-oxo-dG across genomes. Despite their potential, these approaches depend on extensive sequencing coverage and are limited by sequencing errors, coverage biases, and challenges in interpreting strand-specific signals. Additionally, achieving consistent accuracy in resolving strand-specific oxidative events remains a significant challenge, as noted by the authors of these techniques. To overcome these limitations, we developed the Ligation-Dependent Probe Amplification (LPA) assay, a robust alternative for quantitative, strand-specific analysis of 8-oxo-dG and apurinic sites, offering exceptional resolution and sensitivity. Our results show that LPA effectively distinguishes between oxidative damage linked to transcriptional activity and that caused by general oxidative stress.

By capturing strand-specific differences in damage induction and repair kinetics, LPA offers insights into the timing and spatial patterns of oxidative DNA damage. For example, LPA showed that estrogen-driven transcriptional activation causes asymmetric guanine oxidation confined to the actively transcribed strand, with quick, time-sensitive repair processes. In contrast, oxidative stress from H_2O_2 impacts both strands equally and shows a slower repair rate.

The LPA platform offers a versatile framework for dynamically mapping 8-oxo-dG and apurinic site distribution within any DNA region of interest, enabling the reconstruction of repair histories in transcriptionally active domains with unmatched resolution. Notably, our findings highlight that guanine oxidation caused by histone lysine demethylation is not just a byproduct of chromatin remodeling but also acts as a marker of transcriptional activation, specifically targeting transcribed units in a strand- and time-dependent manner. Oxidative damage from external sources like H_2O_2, which is non-transcriptional, results in broader, less selective damage patterns.

In summary, the LPA method presents a new and reliable approach for understanding the link between oxidative DNA damage and transcriptional regulation. By enabling accurate, strand-specific analysis of 8-oxo-dG and apurinic lesions, LPA fills an important methodological gap and provides a new way to explore gene expression control, epigenetic changes, and genome stability under normal and stress conditions.

2. Materials and methods

2.1. Cell culture and treatments

Human breast cancer MCF-7 cells were cultured at 37 °C in a humidified atmosphere containing 5 % CO_2, using Dulbecco's Modified Eagle Medium (DMEM) supplemented with phenol red, L-glutamine (2 mM), insulin (10 μg/ml), hydrocortisone (3.75 ng/ml) and 10 % fetal bovine serum (FBS) (Invitrogen). To assess the effect of estrogen (E2), cells were grown in phenol red-free medium containing 10 % dextran-charcoal-stripped FBS for 1–3 days, then treated with 50 nM E2 for various durations as specified. For positive controls of DNA oxidation, cells were exposed to 0.2 M or 2.0 M H_2O_2 for 30 min.

2.2. 8-oxo-dG immunofluorescence

Immunocytochemistry was performed following the manufacturer's instructions (Trevigen Inc.). The anti-8-oxo-dG monoclonal antibody (clone 15A3) was validated by confocal microscopy [10] and chromatin immunoprecipitation (ChIP) [5]. The signal was resistant to RNase A and sensitive to DNase I. Briefly, cells were fixed for 15 min with methanol at −20 °C, followed by 15 min at −20 °C with acetone. Fixed cells were treated with 0.05 N HCl on ice for 5 min, then incubated with 250 μl of 100 μg/ml RNase A in 150 mM NaCl and 15 mM sodium citrate for 1 h at 37 °C. After washing in PBS and ethanol gradients (35 %, 50 %, 75 %), DNA was denatured in situ with 250 μl of 0.15 N NaOH in 70 % ethanol. DNA was stained with DAPI (Thermo Fisher Scientific; 0.2 μg/ml) for 10 min. Following washes with ethanol and PBS, cells were incubated with 250 μl of blocking buffer (5 % goat serum in PBS) for 1 h at room temperature. Cells were then incubated overnight at 4 °C with the anti-8-hydroxyguanine antibody diluted 1:250 in PBS with 1 % BSA and 0.01 % Tween 20. After washing, cells were incubated with goat anti-mouse IgG conjugated to Alexa Fluor 488 (at 5 μg/ml) for 1 h in the dark. After final washes, cells were mounted with glycerol and observed under a confocal microscope.

2.3. DNA extraction

Genomic DNA was isolated as follows: cell pellets were resuspended in 10 mM Tris-HCl (pH 7.8) and 50 mM NaCl (2×10^7 cells/ml). After adding 1 % SDS, the samples were gently mixed and then incubated overnight at 55 °C with Proteinase K (200 μg/mL). The next day, 70 °C hot NaCl solution (1.5 M) was added to precipitate proteins, followed by phenol-chloroform extraction. DNA was ethanol precipitated, dried and resuspended in TE buffer (10 mM Tris-HCl, 1 mM EDTA, pH 8.0).

2.4. 2D UPLC-MS/MS analysis

Analysis was performed as previously described [49]. DNA hydrolysates were spiked with internal standards: [13C10,15N2]-5-formyl-2′-deoxycytidine (5 fC) and [15N5]-8-oxo-dG at a concentration of 50 fmol/μL. Chromatography was performed using a Waters Acquity 2D UPLC system, equipped with a photodiode array detector (first dimension) and a Xevo TQ-S tandem mass spectrometer (second dimension). The first dimension used a Phenomenex Kinetex C-18 column (150 × 2.1 mm, 1.7 μm), with mobile phases of 0.1 % acetate (A) and acetonitrile (B), employing a gradient elution. The second dimension utilized a Waters X-Select C18 CSH column (30 × 2.1 mm, 1.7 μm) with a similar gradient, but employing methanol as the B solvent. The flow rates were 0.25 mL/min (first dimension) and 0.35 mL/min (second). Data acquisition involved multiple replicates, with transitions optimized via MassLynx software.

2.5. Production of fragments in vitro

Probe design: All probes were designed to hybridize to target

sequences flanking the lesion site, with a melting temperature (Tm) between 58 and 62 °C to ensure specificity. Each probe carried a 5′ phosphate group to enable ligation and non-complementary tail sequences (5–8 nucleotides) were added to the 3′ ends to facilitate subsequent amplification. Primer sequences used for qPCR detection were designed using Primer 3 software, ensuring minimal secondary structure and avoiding complementarity with tail sequences. All oligonucleotides were synthesized by Integrated DNA Technologies (IDT) and purified by HPLC.

In vitro fragment generation was carried out by incubating the DNA with a specific oligo targeting the region of interest and a mixture of nucleotides that included a modified nucleotide (8-oxo-dG or 5 fC), along with High-Fidelity DNA Polymerase at a temperature of 55 °C. Subsequently, the purified and quantified fragments were used again in the ligase reaction. All purifications were performed using standard columns to isolate the amplicons. Note that these fragments are a mixture of a single DNA fragment synthesized in vitro with known percentages of modified nucleotides. This test helps evaluate the method's sensitivity and enzymatic efficiency within a population of heterogeneous fragments. Mass spectrometry analysis of these diverse, stochastic oligonucleotide populations is not informative. Below is an illustration of fragment synthesis which, by its nature, cannot be quantified through LC-MS, as they were not tested for quantity but for specific positions (Fig. S1–S2).

2.6. Ligation-dependent probe amplification (LPA)

The LPA assay, adapted from the Multiplex Ligation-dependent Probe Amplification (MLPA) platform, was optimized to detect oxidative DNA lesions with strand- and sequence-specific resolution. In this study, the approach was applied to identify 8-oxo-7,8-dihydroguanine (8-oxo-dG) and apurinic/apyrimidinic (AP) sites within defined genomic regions.

2.6.1. Preparation and enzymatic digestion

One nanogram of genomic DNA was divided into four aliquots (250 pg each). Two aliquots were treated with Escherichia coli formamidopyrimidine-DNA glycosylase (FpG, 0.01 U; New England Biolabs) for 1 h at 37 °C in Buffer 1 (10 mM Bis-Tris-Propane-HCl, 10 mM $MgCl_2$, 1 mM DTT, pH 7.0) supplemented with BSA. FpG excises oxidized purines (e.g., 8-oxo-dG) and cleaves the DNA backbone at the resulting AP sites, producing a single-nucleotide gap that prevents ligation. The enzyme was inactivated by heating at 98 °C for 5 min, and reactions were stabilized at 40 °C. Control samples (undigested DNA) were treated with FpG storage buffer only.

2.6.2. Probe design, phosphorylation and annealing

For each target region, two probe pairs were designed: one specific to the plus strand [Right Probe Oligonucleotide (RPO +) and Left Probe Oligonucleotide (LPO +)] and one to the minus strand [RPO (−) and LPO (−)]. The 5′ ends of RPO probes were phosphorylated using T4 polynucleotide kinase (20 U, 100 nM ATP, 45 min at 37 °C), followed by inactivation at 65 °C for 10 min, to enable efficient ligation. Probes (12.5 fmol/sample) were combined with 5 × KCl buffer (750 mM KCl, 50 mM Tris-HCl pH 8.0, 5 mM EDTA), denatured at 95 °C for 1 min, and annealed to the DNA at 60 °C for 2 h.

2.6.3. Ligation reaction

Annealed probes were ligated using SALSA Ligase-65 (MRC Holland), a thermostable NAD-dependent ligase, in a 60 μL reaction containing dilution buffer (5 mM Tris-HCl pH 8.5, 2.6 mM $MgCl_2$, 0.013 % Triton X-100, 0.2 mM NAD) and 1 U ligase. Ligation was performed at 54 °C for 1 h, followed by enzyme inactivation at 98 °C for 15 min.

2.6.4. Quantitative PCR amplification

Ten microliters of ligation products were amplified by qPCR using FastStart Universal SYBR Green Master (Rox) (Roche) on a 7500 Real-Time PCR System (Applied Biosystems) with the following cycling conditions: 95 °C for 10 min; 35 cycles of 95 °C for 30 s, 60 °C for 30 s, and 72 °C for 40 s; and a final extension at 72 °C for 10 min. Universal primers (5′F: GGGTTCCCTAAGGGTTGG; 3′R: GTGCCAGCAAGATCCAATCTAGA) were complementary to constant tail sequences present in all probes, enabling multiplexed amplification.

2.6.5. Data interpretation

In the LPA system, intact target sites allow efficient ligation and amplification, whereas oxidative lesions or AP sites block probe ligation, resulting in reduced qPCR signal. By comparing amplification in FpG-treated versus untreated samples, lesion frequency can be quantified with single-nucleotide positional and strand-specific resolution.

2.6.6. Validation and controls

Synthetic DNA fragments containing defined percentages (0, 20, 40 and 60 %) of 8-oxo-dG or 5-formylcytosine were used to validate the assay's sensitivity, enzymatic efficiency, and linearity. Control reactions confirmed that FpG digestion selectively abolished ligation at modified sites, consistent with its N-glycosylase and AP-lyase activities.

In this system, oxidative lesions such as 8-oxo-dG or AP sites prevent ligation, resulting in reduced PCR amplification. The difference in amplification between digested and undigested samples allows quantitative, strand-specific lesion mapping with high positional resolution (**Graphical Abstract**).

2.7. RNA extraction, qRT-PCR and qPCR

Total RNA was isolated using Trizol (Gibco/Invitrogen). cDNA synthesis was performed using 1 μg of RNA, with SuperScript III (Invitrogen) and random hexamers and incubated at 50 °C for 1 h. The reaction was then heat-inactivated at 70 °C for 15 min qRT-PCR and qPCR were conducted on a 7500 system with SYBR Green detection. Primer sequences for *TFF1* and 18S are below. Results were normalized to 18S expression.

2.7.1. Primer sequences used are

TFF1 F: 5′-CCAGACAGAGACGTGTACAGT-3′
TFF1 R: 5′-ATTCACACTCCTCTTCTGGA-3'.
18S F: 5′-GACCGATGTATATGCTTGCAGAGT-3′,
18S R: 5′-GGATCTGGAGTTAAACTGGTCCAG-3'.

2.8. Statistical analysis

Data are expressed as means ± SEM. Statistical significance was evaluated using one-way ANOVA with Bonferroni post hoc testing, with $P < 0.05$ considered significant. Analyses were performed with JMP 7.1 software (SAS). Additional details are available in the Supplementary Data.

3. Results

3.1. Detection of oxidative damage via 8-oxo-dG and apurinic site formation

Excess reactive oxygen species (ROS) induce oxidative stress, compromising genome stability by causing chemical modifications in DNA. Among these, small base lesions are most frequent and are typically repaired via the base excision repair (BER) pathway, producing apurinic/apyrimidinic (AP) sites as intermediates. ROS preferentially target purines due to their lower redox potential [20], leading to highly mutagenic lesions such as 7,8-dihydro-8-oxoguanine (oxoG) and 7, 8-dihydro-8-oxoadenine (oxoA). These lesions are the predominant signatures of oxidative DNA damage, with guanine being significantly more prone to oxidation than adenine. On average, each human cell

accumulates approximately 10,000 such lesions daily [21]. Notably, oxoA occurs at roughly one-tenth the frequency of oxoG, reflecting the higher redox potential of adenine [22].

To detect 8-oxo-dG and AP sites with strand and sequence specificity, we developed a ligation-dependent probe amplification (LPA) technique. This method leverages two key enzymes: FpG (formamidopyrimidine-DNA glycosylase), which recognizes and excises oxidized purines including 8-oxo-dG and Ligase-65, a thermostable NAD-dependent DNA ligase. FpG possesses both N-glycosylase and AP-lyase activities, recognizing a range of oxidized purines and some oxidized pyrimidines [23,24]. Following excision, FpG cleaves the DNA backbone at the AP site, creating a single-nucleotide gap that blocks ligation and subsequent amplification unless the lesion is repaired or bypassed. This mechanistic feature distinguishes LPA from techniques without single-nucleotide resolution. This activity further distinguishes oxidative modifications involved in epigenetic regulation from those representing damage, as the former are transient and rapidly processed.

Ligase-65, derived from bacterial strain MRCH-0065, is highly efficient at sealing nicks between perfectly matched oligonucleotides annealed to DNA at high temperatures (54–65 °C). Its activity drops sharply with mismatched termini, providing specificity [25]. It is fully inactivated by a brief incubation at 98 °C, facilitating downstream processing.

Our LPA protocol begins with denaturation and hybridization of target DNA to probes containing the guanine(s) of interest (Fig. 1). FpG treatment introduces single-nucleotide gaps at oxidized guanines, preventing probe ligation. Ligase-65 then selectively seals intact probes, enabling PCR amplification only at undamaged sites. This approach enables the strand-specific, quantitative detection of 8-oxo-dG and AP sites with high positional resolution.

3.2. Assessment of the efficiency of LPA through chemical DNA oxidation

To evaluate LPA performance, MCF7 cells were exposed to vehicle, 0.2 M, or 2.0 M H_2O_2 for 30 min H_2O_2 induces widespread oxidative DNA damage, including single- and double-strand breaks [26]. Immunofluorescence analysis confirmed dose-dependent formation of 8-oxo-dG foci (Fig. 2A). Parallel LPA analysis of the *TFF1* gene showed increased damage signals correlating with H_2O_2 dose (Fig. 2B). Without FpG, the LPA signal decreased with higher H_2O_2, reflecting increased guanine oxidation and subsequent removal, which generates AP sites that hinder probe ligation [27]. When FpG was included, the damage

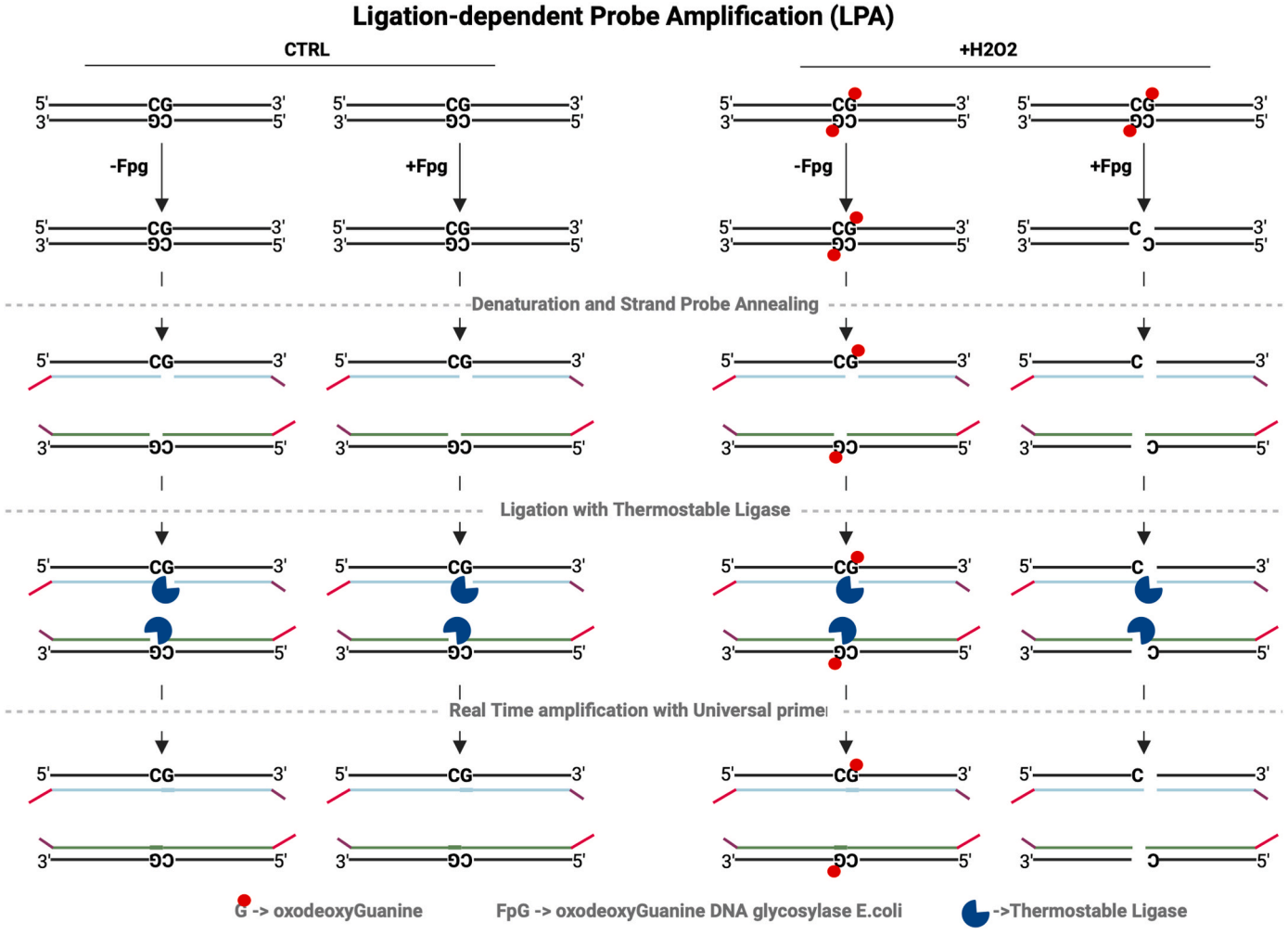

Fig. 1. Overview of the LPA protocol for strand-specific quantification of 8-oxo-dG.
Schematic illustration of the Ligation-Dependent Probe Amplification (LPA) workflow. The assay begins with genomic DNA that may contain 8-oxo-dG lesions (represented by red circles). Samples are treated with or without formamidopyrimidine-DNA glycosylase (FpG), which recognizes and excises 8-oxo-dG, creating abasic (AP) sites. Strand-specific probes are then annealed to the target DNA. A thermostable ligase joins the probes only if they are perfectly matched to the DNA sequence, i.e., if no AP sites are present. Finally, quantitative PCR (qPCR) is used to amplify the ligated products, with the resulting signal inversely proportional to the amount of oxidative damage present in the sample. Created with BioRender.com.

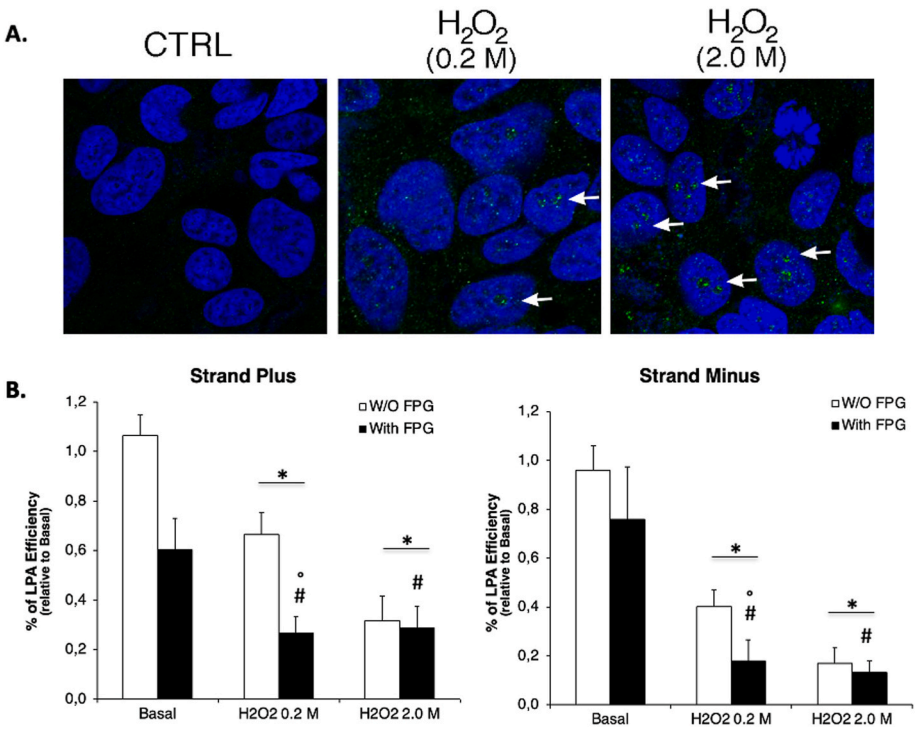

Fig. 2. LPA efficiency in detecting 8-oxo-dG following hydrogen peroxide (H_2O_2) treatment.
Immunofluorescence images showing 8-oxo-dG (green) in MCF7 cells treated with vehicle (CTRL), 0.2 M H_2O_2 and 2.0 M H_2O_2 for 30 min. Nuclear DNA was counterstained with DAPI (blue). White arrows indicate representative 8-oxo-dG foci. Note the dose-dependent increase in 8-oxo-dG foci with increasing H_2O_2 concentration. The intensity of the green fluorescence is proportional to the amount of 8-oxo-dG present. (B) Quantitative analysis of LPA efficiency for both DNA strands (Strand Plus and Strand Minus) in MCF7 cells treated with 0.2 M and 2.0 M H_2O_2, with and without pre-treatment with FpG. The LPA efficiency is expressed as a percentage relative to the basal condition (cells treated with vehicle). In the absence of FpG (black bars), LPA efficiency decreases with increasing H_2O_2 concentration, indicating increased oxidative damage. Pre-treatment with FpG (white bars) normalizes the LPA signal, suggesting that FpG removes 8-oxo-dG, allowing for probe ligation. Statistical significance was assessed using the Mann-Whitney test: *P < 0.05 vs. basal without FpG, #P < 0.05 vs. basal with FpG, °P < 0.05 between conditions within the same sample.

was effectively excised, normalizing the signals across doses, indicating robust detection of guanine oxidation and repair kinetics (Fig. 2B).

These results support the capacity of LPA to detect strand-specific oxidative damage and repair dynamics with high resolution.

3.3. LPA detects oxidized purines but not oxidized pyrimidines

After visualizing 8-oxo-dG and AP sites in H_2O_2-treated cells, we next assessed the sensitivity of LPA to defined levels of oxidative DNA damage. To do this, we generated in vitro DNA fragments of the *TFF1* gene containing known proportions of 8-oxo-dG—specifically, 20 %, 40 %, or 60 % modified guanines—on either the plus or minus strand (see Methods). As anticipated, increasing the proportion of 8-oxo-dG led to a progressive decrease in the LPA signal (Fig. 3A), reflecting impaired probe ligation due to the presence of oxidative lesions.

This reduction was even more pronounced when FpG was included in the reaction. Since FpG cleaves at oxidized purines, its presence revealed the full extent of damage, especially when 8-oxo-dGs were located at or near adjacent positions. In such cases, DNA integrity was severely compromised, resulting in poor amplification efficiency by LPA.

FpG functions as an N-glycosylase that recognizes and removes a broad spectrum of damaged bases, including 8-oxo-dG, 8-oxoadenine, fapy-guanine, methyl-fapy-guanine, fapy-adenine, aflatoxin B1-fapy-guanine, 5-hydroxycytosine and 5-hydroxyuracil [28,29]. Among other oxidized bases, 5-hydroxymethylcytosine (5hmC) is of particular interest due to its short genomic half-life, as it is rapidly converted into 5-formylcytosine (5 fC) and 5-carboxylcytosine (5caC) by TET enzymes. These oxidized derivatives are ultimately replaced with unmodified cytosines via the base excision repair (BER) pathway [30]. While 5 fC can function as a stable epigenetic mark [31], our analysis of synthetic DNA fragments containing 40 % 5 fC revealed no detectable LPA signal (Fig. 3B). This suggests that LPA, under the conditions used here, is specific for 8-oxo-dG and does not detect oxidized cytosine derivatives like 5 fC.

In summary, our data demonstrate that LPA reliably detects and quantifies 8-oxo-dG and AP sites at single-nucleotide resolution. FpG treatment significantly reduces LPA amplification efficiency even in fragments containing a single oxidized guanine, whereas modified cytosines, including 5 fC, do not interfere with LPA performance. This highlights the specificity and accuracy of LPA for mapping guanine oxidation events.

3.4. Transcription initiation is accompanied by strand-specific G oxidation

DNA repair enzymes are actively recruited during the early stages of transcriptional activation, often in conjunction with localized bursts of oxidative stress at promoters and enhancers [28]. Among the DNA bases, guanine is particularly susceptible to oxidation and accumulating evidence suggests that this modification serves not simply as damage but as a biochemical signal associated with transcription initiation [29,30].

To investigate this, we applied LPA to map oxidative modifications at the estrogen-responsive *TFF1* gene. Upon treatment with estrogen (E2), we observed the rapid formation of nuclear foci containing 8-oxo-dG, as detected by immunofluorescence (Fig. 4A) and confirmed by mass spectrometry (Fig. S3). Oxidative modifications of both guanine and cytosine residues were detectable as early as 15 min after treatment and

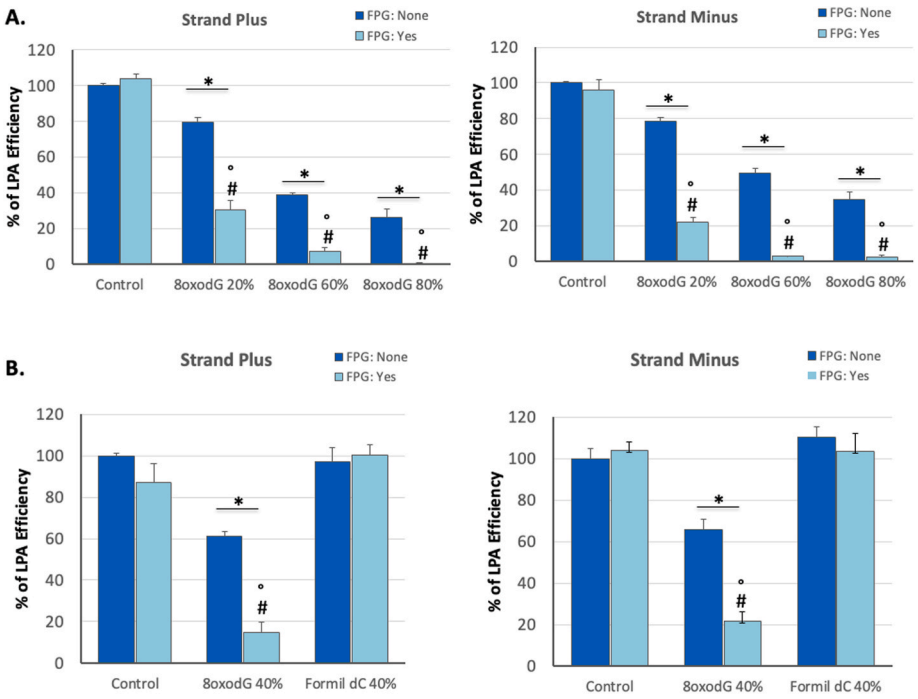

Fig. 3. LPA specificity for 8-oxo-dG over 5-formylcytosine (5 fC).
(A) Strand-specific detection of 8-oxo-dG damage in in vitro-generated DNA fragments containing varying levels of 8-oxo-dG (20 %, 60 %, 80 %) in the presence (light blue) or absence (dark blue) of FpG. LPA efficiency is expressed as a percentage of the signal from control fragments without modifications
(B) Evaluation of LPA specificity in detecting 8-oxo-dG versus 5 fC (40 %) incorporated into in vitro fragments, with (light blue) or without (dark blue) FpG. Strand Plus e Strand Minus rappresentano i due filamenti di DNA. LPA efficiency is expressed as a percentage of the signal from control fragments without modifications. Note that FpG treatment significantly reduces the LPA signal only in fragments containing 8-oxo-dG, but not in fragments containing 5 fC. Statistical significance was determined using the Mann-Whitney test: *P < 0.05 indicates a significant difference between samples with and without FpG, #P < 0.05 indicates a significant difference compared to Control fragments without modifications and °P < 0.05 indicates a significant difference between conditions within the same sample.

persisted up to 60 min, consistent with a regulated oxidative event occurring during gene activation (Fig. 4B and Fig. S3–S4).

Time-course LPA analyses revealed strand-specific oxidation dynamics. On the minus (−) strand, guanine oxidation was detectable within 5 min of E2 exposure and appeared to be largely repaired by 15 min. In contrast, the plus (+) strand showed oxidation starting between 5 and 15 min, with peak repair observed at 30 min (Fig. 4C). This temporal asymmetry between the two strands suggests that oxidative modifications occur in a transcription-dependent manner—possibly reflecting the formation of a transcription loop or bubble—and that these oxidative marks may align with the 5′–3′ direction of transcription [31].

Altogether, these findings support the view that oxidative DNA modifications, particularly 8-oxo-dG, are not merely byproducts of cellular stress but may serve as dynamic, strand-specific epigenetic signals that help coordinate gene activation and regulation.

4. Discussion

The accurate detection of oxidative DNA lesions, particularly 8-oxo-7,8-dihydroguanine (8-oxo-dG), remains a critical challenge in molecular biology due to the limitations of current methodologies in resolution, specificity and artifact control. Techniques such as GC-MS, LC-MS, ELISA, immunofluorescence and comet assays, while widely used, often lack the precision needed to localize lesions at single-nucleotide resolution or to monitor the kinetics of DNA repair in real time [32–34]. Moreover, these methods are susceptible to artifacts introduced during sample preparation—such as spurious oxidation during high-temperature derivatization steps in GC-MS—which can significantly skew results [35–37].

To overcome these limitations, we developed the Ligation-based Proximity Assay (LPA). This strand-specific and highly sensitive technique enables the detection and quantification of 8-oxo-dG and apurinic (AP) sites at single-nucleotide resolution. Our validation experiments demonstrated that LPA accurately identifies physiologically relevant oxidative DNA damage, whether induced by exogenous agents like H_2O_2 or by endogenous processes such as transcriptional activation. Notably, LPA revealed asymmetric patterns of guanine oxidation and rapid repair on the transcribed strand, highlighting the method's ability to capture the dynamics of oxidative stress and base excision repair (BER) activity in situ.

The asymmetry observed, with earlier oxidation and faster repair on the minus strand, points to a role for these modifications in defining transcriptional polarity and potentially promoting transcription loop formation [41].

Our findings support the hypothesis that oxidative lesions, particularly 8-oxo-dG, may function not solely as genomic damage but also as regulatory elements associated with transcriptional activity [38–40]. For instance, in estrogen-stimulated MCF7 cells—selected for their precisely timed transcriptional response—we observed temporally coordinated and strand-specific guanine and cytosine oxidation at the *TFF1* promoter—consistent with a regulated oxidative burst during gene activation. The observed asymmetry, with earlier oxidation and faster repair on the minus strand, suggests a functional role for oxidative modifications in defining transcriptional polarity and potentially promoting transcription loop formation [41].

Despite these advances, several caveats must be considered. First, the presence of guanine-rich sequences at gene promoters and termini introduces the possibility of G-quadruplex (G4) formation—secondary DNA structures known to influence both damage susceptibility and detection. G4s can stabilize R-loops and modulate the accessibility of DNA repair enzymes, potentially confounding the interpretation of

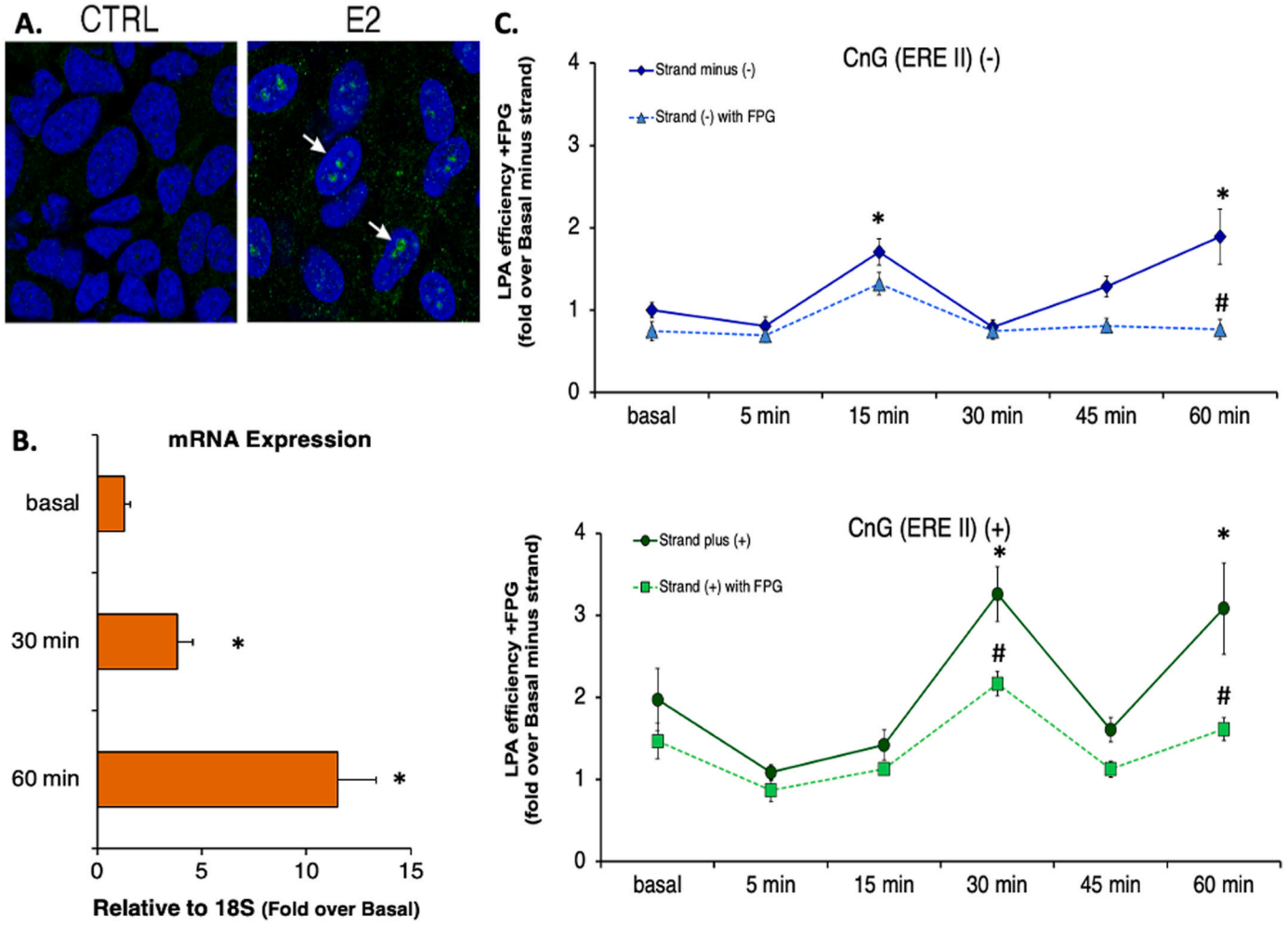

Fig. 4. Estrogen-induced strand-specific DNA oxidation and *TFF1* gene expression in MCF7 cells.
Immunofluorescence images depicting 8-oxo-dG (green) in MCF7 cells treated with vehicle (CTRL) or 50 nM estrogen (E2) for 30 min. Nuclear DNA was visualized with DAPI (blue). White arrows indicate representative 8-oxo-dG foci. (B) *TFF1* gene expression levels, measured by qRT-PCR, following estrogen stimulation at 30 and 60 min. Expression levels are normalized to 18S rRNA and expressed as fold change over basal (vehicle-treated cells). Asterisks (*) indicate statistically significant differences compared to the basal condition. (C) Strand-specific detection of 8-oxo-dG damage and repair at the *TFF1* estrogen response element (ERE) CnG site over time (5, 15, 30, 45, 60 min) in the presence (dashed lines) and absence (solid lines) of FpG. Strand minus (−) and Strand plus (+) report values of LPA efficiency at the site of interest for each strand. Statistical significance was assessed using the Mann-Whitney test. *P $<$ 0.05 indicates a significant difference compared to basal without FpG and #P $<$ 0.05 indicates a statistically significant difference between conditions at the same time point.

strand-specific oxidative signals [42–46]. These topological features may lead to underestimation or mislocalization of lesions, particularly when standard antibodies or detection probes are not optimized for binding within complex DNA conformations [47].

Second, the enzymatic specificity of formamidopyrimidine-DNA glycosylase (FpG), the key component of our assay, presents an interpretive limitation. Although FpG effectively excises 8-oxo-dG, it also targets other oxidized purine derivatives, including fapy-guanine, fapy-adenine and ring-opened guanine structures [24,48]. As a result, the LPA signal may represent a composite of multiple oxidative lesions, complicating efforts to attribute observed damage exclusively to 8-oxo-dG—particularly in structurally dynamic regions such as G4s.

These limitations are not unique to LPA. Similar challenges affect other lesion mapping approaches, including AP-seq, Click-code-seq and nanopore-based detection methods [19], all of which may struggle to resolve damage within G4-rich or transcriptionally active regions with high precision.

To strengthen the interpretation of LPA data, we recommend combining it with complementary techniques such as LC-MS/MS, chromatin immunoprecipitation followed by sequencing (ChIP-seq) and G4-specific antibodies. Table 1 provides a comparative overview of available methods, outlining their relative strengths and constraints when used to study oxidative lesions at high resolution.

In conclusion, LPA represents a robust, rapid and cost-effective method for mapping oxidative DNA damage and repair with strand and nucleotide specificity. Its ability to resolve lesion dynamics in transcriptionally active chromatin opens new avenues for investigating the regulatory roles of oxidative modifications in gene expression. While structural and enzymatic constraints must be considered, the assay's performance in both experimental and physiological settings highlights its potential as a valuable tool for genome stability research and epigenetic regulation studies.

CRediT authorship contribution statement

Antonella Romano: Formal analysis, Methodology, Validation, Writing – original draft, Writing – review & editing, Visualization, Data curation. **Antonia Feola:** Data curation, Formal analysis, Investigation, Methodology, Validation, Writing – original draft, Writing – review & editing, Visualization. **Valentina Morgera:** Formal analysis, Methodology, Writing – original draft, Writing – review & editing, Visualization. **Alfonso Tramontano:** Data curation, Formal analysis, Investigation,

Table 1
Comparison of methods for detecting oxidative DNA damage.

Method	Principle	Advantages	Disadvantages	Strand Specificity	Single-Nucleotide Resolution	Redox Biology Focus	Key References
LPA (This Study)	Strand-specific probe ligation, FpG digestion, qPCR amplification	High sensitivity, strand-specific, high resolution, quantitative, flexible	Limited to known sequences, FpG recognizes multiple lesions, G4 structures interfere	Yes	Yes	Captures dynamics of redox-mediated transcription	N/A
GC-MS/LC-MS/MS	Quantification of modified bases via mass spectrometry	High sensitivity, quantitative, direct measurement	Can introduce artifacts during sample preparation, lacks spatial resolution, complex derivatization	No	No	Direct quantification of 8-oxo-dG	Gackowski D et al. Anal Chem. 2016, 88 (24):12128–12136.
ELISA/ Immunofluorescence	Antibody-based detection of modified bases	Relatively simple, accessible, high-throughput potential	Limited resolution, potential for cross-reactivity, indirect measurement	No	No	Provides general assessment of oxidative stress	Chao MR et al. Redox Biol. 2021; 42:101872.
Comet Assay (±FpG)	Electrophoretic separation of DNA fragments, visual assessment of DNA damage	Relatively simple, sensitive to DNA breaks, can be modified to detect oxidative damage	Subjective, limited resolution, reproducibility issues, does not provide strand-specific information	No	No	Provides general assessment of DNA damage	Dunkelberger L et al. Methods Mol Biol. 2022; 2422:263–269.
AP-Seq	Genome-wide mapping of apurinic/apyrimidinic sites following chemical treatment and sequencing	Genome-wide coverage, nucleotide resolution	Requires deep sequencing, chemical treatment may introduce artifacts, challenging to achieve strand specificity	Limited	Yes	Provides a snapshot of AP site distribution	Poetsch AR. Methods Mol Biol. 2020; 2175:95–108.
Click-Code-Seq	Nucleotide-resolution mapping of 8-oxo-dG via click chemistry and sequencing	Genome-wide coverage, nucleotide resolution	Requires chemical modification, sequencing errors, complex data analysis, challenges in achieving reliable strand specificity	Limited	Yes	Useful for mapping redox-sensitive regions within the genome	Wu J et al. J Am Chem Soc. 2018 Aug 8; 140 (31):9783–9787.
Nanopore Sequencing	Direct DNA sequencing that can detect base modifications without amplification or labeling	Real-time analysis, potential for direct detection of modified bases, long read lengths	High error rate, complex data analysis, limited throughput	Potential	Potential	Emerging technology with potential applications in redox biology	Pagès-Gallego M et al. Nat Commun. 2025 Jun 5; 16 (1):5236

Table 1: **Comparison of Methods for Detecting Oxidative DNA Damage**. This table summarizes the principle, advantages, disadvantages, strand specificity, resolution, and redox biology focus of the Ligation-Dependent Probe Amplification (LPA) assay, along with other common methods for detecting oxidative DNA damage. Key references are provided for further information on each technique.

Methodology, Visualization, Writing – original draft, Writing – review & editing. **Samantha Messina:** Supervision, Validation, Writing – original draft, Writing – review & editing. **Daniel Gackowski:** Data curation, Formal analysis, Investigation, Methodology, Writing – original draft, Writing – review & editing. **Ewelina Zarakowska:** Data curation, Formal analysis, Investigation, Methodology, Visualization, Writing – original draft, Writing – review & editing. **Ryszard Olinski:** Data curation, Formal analysis, Investigation, Methodology, Supervision, Validation, Writing – original draft, Writing – review & editing. **Vittorio Enrico Avvedimento:** Conceptualization, Investigation, Methodology, Supervision, Validation, Visualization, Writing – original draft, Writing – review & editing. **Candida Zuchegna:** Conceptualization, Data curation, Formal analysis, Investigation, Methodology, Supervision, Validation, Writing – original draft, Writing – review & editing. **Antonio Porcellini:** Conceptualization, Data curation, Formal analysis, Investigation, Methodology, Supervision, Validation, Visualization, Writing – original draft, Writing – review & editing. **Antonio Pezone:** Conceptualization, Funding acquisition, Investigation, Methodology, Supervision, Writing – review & editing, Validation, Visualization, Writing – original draft.

Ethics statement

Not applicable.

Funding

This research was funded by the University of Naples "Federico II," acquired by Prof. Pezone (FRA2022).

Declaration of competing interest

The authors declare that they have no known competing financial interests or personal relationships that could have appeared to influence the work reported in this paper.

Acknowledgments

We thank the University of Naples Federico II for funding our research and Dr. Rita Cirillo for her expert technical assistance.

Appendix. ASupplementary data

Supplementary data to this article can be found online at https://doi.org/10.1016/j.redox.2025.103842.

Abbreviations

8-oxo-dG 8-oxo-7,8-dihydroguanine
AP site Apurinic
BER Base Excision
DAPI 4′,6-Diamidino-2
DSB Double-Strand Break
ELISA Enzyme-Linked Immunosorbent
ERE Estrogen Response
EtOH Ethanol
E2 17β-Estradiol (Estrogen
FpG Formamidopyrimidine-DNA Glycosylase
GC-MS Gas Chromatography–Mass Spectrometry
G4 G-quadruplex
H_2O_2 Hydrogen Peroxide
LC-MS Liquid Chromatography–Mass Spectrometry
LPA Ligation-Dependent Probe Amplification
LPO Left Probe Oligonucleotide
MLPA Multiplex Ligation-dependent Probe Amplification
MS Mass Spectrometry

NAD	Nicotinamide Adenine Dinucleotide
NER	Nucleotide Excision Repair
OGG1	8-oxo-dG DNA Glycosylase 1
PCR/qPCR	Polymerase Chain Reaction/Quantitative PCR
PolyA	Polyadenylation
RPO	Right Probe Oligonucleotide
ROS	Reactive Oxygen Species
RT-qPCR/qRT-PCR	Reverse Transcription Quantitative PCR
SEM	Standard Error of the Mean
SSB	Single-Strand Break
TET	Ten-Eleven Translocation Enzymes
TOPIIβ	Topoisomerase II Beta
TFF1	Trefoil Factor 1 (gene)
UPLC	Ultra-Performance Liquid Chromatography
5 fC	5-Formylcytosine
5hmC	5-Hydroxymethylcytosine
5hmU	5-Hydroxyuracil
5caC	5-Carboxylcytosine

Data availability

Data will be made available on request.

References

[1] J.Y. Hahm, J. Park, E.S. Jang, S.W. Chi, 8-Oxoguanine: from oxidative damage to epigenetic and epitranscriptional modification, Exp. Mol. Med. 54 (10) (2022) 1626–1642, https://doi.org/10.1038/s12276-022-00822-z.

[2] F. Zhao, J. Zhu, L. Shi, X. Wu, OGG1 in the kidney: beyond base excision repair, Oxid. Med. Cell. Longev. 2022 (2022) 5774641, https://doi.org/10.1155/2022/5774641. Published 2022 Dec 30.

[3] A.L. Jacobs, P. Schär, DNA glycosylases: in DNA repair and beyond, Chromosoma 121 (1) (2012) 1–20, https://doi.org/10.1007/s00412-011-0347-4.

[4] B. Perillo, M.N. Ombra, A. Bertoni, et al., DNA oxidation as triggered by H3K9me2 demethylation drives estrogen-induced gene expression, Science 319 (5860) (2008) 202–206, https://doi.org/10.1126/science.1147674.

[5] A. Pezone, C. Zuchegna, A. Tramontano, et al., RNA stabilizes transcription-dependent chromatin loops induced by nuclear hormones, Sci. Rep. 9 (1) (2019) 3925, https://doi.org/10.1038/s41598-019-40123-6. Published 2019 Mar 8.

[6] C. Zuchegna, F. Aceto, A. Bertoni, et al., Mechanism of retinoic acid-induced transcription: histone code, DNA oxidation and formation of chromatin loops [published correction appears in nucleic acids res. 2014 Oct 29;42(19):12329], Nucleic Acids Res. 42 (17) (2014) 11040–11055, https://doi.org/10.1093/nar/gku823.

[7] B. Perillo, A. Tramontano, A. Pezone, A. Migliaccio, LSD1: more than demethylation of histone lysine residues, Exp. Mol. Med. 52 (12) (2020) 1936–1947, https://doi.org/10.1038/s12276-020-00542-2.

[8] S. Sengupta, H. Wang, C. Yang, B. Szczesny, M.L. Hegde, S. Mitra, Ligand-induced gene activation is associated with oxidative genome damage whose repair is required for transcription, Proc. Natl. Acad. Sci. U. S. A. 117 (36) (2020) 22183–22192, https://doi.org/10.1073/pnas.1919445117.

[9] S. Amente, A. Bertoni, A. Morano, L. Lania, E.V. Avvedimento, B. Majello, LSD1-mediated demethylation of histone H3 lysine 4 triggers Myc-induced transcription, Oncogene 29 (25) (2010) 3691–3702, https://doi.org/10.1038/onc.2010.120.

[10] A. Pezone, M.L. Taddei, A. Tramontano, et al., Targeted DNA oxidation by LSD1-SMAD2/3 primes TGF-β1/EMT genes for activation or repression, Nucleic Acids Res. 48 (16) (2020) 8943–8958, https://doi.org/10.1093/nar/gkaa599.

[11] W. Kong, Y. Zhao, X. Dai, C. You, Methodologies for the detection and sequencing of the epigenetic-like oxidative DNA modification, 8-oxo-7,8-dihydroguanine, Mutat. Res. Rev. Mutat. Res. 794 (2024) 108516, https://doi.org/10.1016/j.mrrev.2024.108516.

[12] M.P. Murphy, H. Bayir, V. Belousov, et al., Guidelines for measuring reactive oxygen species and oxidative damage in cells and in vivo, Nat. Metab. 4 (6) (2022) 651–662, https://doi.org/10.1038/s42255-022-00591-z.

[13] T. Detinis Zur, J. Deek, Y. Ebenstein, Single-molecule approaches for DNA damage detection and repair: a focus on Repair Assisted Damage Detection (RADD), DNA Repair 129 (2023) 103533, https://doi.org/10.1016/j.dnarep.2023.103533.

[14] A.R. Poetsch, The genomics of oxidative DNA damage, repair and resulting mutagenesis, Comput. Struct. Biotechnol. J. 18 (2020) 207–219, https://doi.org/10.1016/j.csbj.2019.12.013. Published 2020 Jan 7.

[15] M.R. Chao, M.D. Evans, C.W. Hu, et al., Biomarkers of nucleic acid oxidation - a summary state-of-the-art, Redox Biol. 42 (2021) 101872, https://doi.org/10.1016/j.redox.2021.101872.

[16] Z. Chen, J. Shi, Y. Zhang, S. Han, J. Zhang, G. Jia, DNA oxidative damage as a sensitive genetic endpoint to detect the genotoxicity induced by titanium dioxide nanoparticles, Nanomaterials 12 (15) (2022) 2616, https://doi.org/10.3390/nano12152616. Published 2022 Jul 29.

[17] A.R. Poetsch, AP-Seq: a method to measure apurinic sites and small base adducts genome-wide, Methods Mol. Biol. 2175 (2020) 95–108, https://doi.org/10.1007/978-1-0716-0763-3_8. PMID: 32681486.

[18] J. Wu, M. McKeague, S.J. Sturla, Nucleotide-resolution genome-wide mapping of oxidative DNA damage by click-code-seq, J. Am. Chem. Soc. 140 (31) (2018 Aug 8) 9783–9787, https://doi.org/10.1021/jacs.8b03715. Epub 2018 Jul 26. PMID: 29944356.

[19] M. Pagès-Gallego, D.M.K. van Soest, N.J.M. Besselink, R. Straver, J.P. Keijer, C. Vermeulen, A. Marcozzi, M.J. van Roosmalen, R. van Boxtel, B.M.T. Burgering, T.B. Dansen, J. de Ridder, Direct detection of 8-oxo-dG using nanopore sequencing, Nat. Commun. 16 (1) (2025 Jun 5) 5236, https://doi.org/10.1038/s41467-025-60391-3. PMID: 40473638; PMCID: PMC12141616.

[20] R. De Bont, N. van Larebeke, Endogenous DNA damage in humans: a review of quantitative data, Mutagenesis 19 (3) (2004 May) 169–185, https://doi.org/10.1093/mutage/geh025. PMID: 15123782.

[21] A.L. Rozelle, Y. Cheun, C.K. Vilas, M.C. Koag, S. Lee, DNA interstrand cross-links induced by the major oxidative adenine lesion 7,8-dihydro-8-oxoadenine, Nat. Commun. 12 (1) (2021 Mar 26) 1897, https://doi.org/10.1038/s41467-021-22273-2. PMID: 33772030; PMCID: PMC7997976.

[22] J. Cadet, K.J.A. Davies, M.H. Medeiros, P. Di Mascio, J.R. Wagner, Formation and repair of oxidatively generated damage in cellular DNA, Free Radic. Biol. Med. 107 (2017 Jun) 13–34, https://doi.org/10.1016/j.freeradbiomed.2016.12.049. Epub 2017 Jan 2. PMID: 28057600; PMCID: PMC5457722.

[23] J.P. Schouten, C.J. McElgunn, R. Waaijer, D. Zwijnenburg, F. Diepvens, G. Pals, Relative quantification of 40 nucleic acid sequences by multiplex ligation-dependent probe amplification, Nucleic Acids Res. 30 (12) (2002) e57, https://doi.org/10.1093/nar/gnf056.

[24] J. Tchou, V. Bodepudi, S. Shibutani, et al., Substrate specificity of Fpg protein. Recognition and cleavage of oxidatively damaged DNA, J. Biol. Chem. 269 (21) (1994) 15318–15324.

[25] Z. Hatahet, Y.W. Kow, A.A. Purmal, R.P. Cunningham, S.S. Wallace, New substrates for old enzymes. 5-Hydroxy-2'-deoxycytidine and 5-hydroxy-2'-deoxyuridine are substrates for Escherichia coli endonuclease III and formamidopyrimidine DNA N-glycosylase, while 5-hydroxy-2'-deoxyuridine is a substrate for uracil DNA N-glycosylase, J. Biol. Chem. 269 (29) (1994) 18814–18820.

[26] M. Bachman, S. Uribe-Lewis, X. Yang, H.E. Burgess, M. Iurlaro, W. Reik, A. Murrell, S. Balasubramanian, 5-Formylcytosine can be a stable DNA modification in mammals, Nat. Chem. Biol. 11 (8) (2015 Aug) 555–557, https://doi.org/10.1038/nchembio.1848. Epub 2015 Jun 22. PMID: 26098680; PMCID: PMC5486442.

[27] G.A. Santa-Gonzalez, A. Gomez-Molina, M. Arcos-Burgos, J.N. Meyer, M. Camargo, Distinctive adaptive response to repeated exposure to hydrogen peroxide associated with upregulation of DNA repair genes and cell cycle arrest, Redox Biol. 9 (2016) 124–133, https://doi.org/10.1016/j.redox.2016.07.004.

[28] J. Nakamura, E.R. Purvis, J.A. Swenberg, Micromolar concentrations of hydrogen peroxide induce oxidative DNA lesions more efficiently than millimolar concentrations in mammalian cells, Nucleic Acids Res. 31 (6) (2003 Mar 15) 1790–1795, https://doi.org/10.1093/nar/gkg263. PMID: 12626721; PMCID: PMC152865.

[29] R. Gilboa, D.O. Zharkov, G. Golan, et al., Structure of formamidopyrimidine-DNA glycosylase covalently complexed to DNA, J. Biol. Chem. 277 (22) (2002) 19811–19816, https://doi.org/10.1074/jbc.M202058200.

[30] S.L. Wu, L. Yang, C. Huang, et al., Genome-wide characterization of dynamic DNA 5-hydroxymethylcytosine and TET2-related DNA demethylation during breast tumorigenesis, Clin. Epigenet. 16 (1) (2024) 125, https://doi.org/10.1186/s13148-024-01726-7. Published 2024 Sep. 11.

[31] E.A. Raiber, P. Murat, D.Y. Chirgadze, D. Beraldi, B.F. Luisi, S. Balasubramanian, 5-Formylcytosine alters the structure of the DNA double helix, Nat. Struct. Mol. Biol. 22 (1) (2015) 44–49, https://doi.org/10.1038/nsmb.2936.

[32] H. Bunch, Role of genome guardian proteins in transcriptional elongation, FEBS Lett. 590 (8) (2016) 1064–1075, https://doi.org/10.1002/1873-3468.12152.

[33] W. Cai, C. Xiao, T. Fan, et al., Targeting LSD1 in cancer: molecular elucidation and recent advances, Cancer Lett. 598 (2024) 217093, https://doi.org/10.1016/j.canlet.2024.217093.

[34] B. Perillo, M. Di Donato, A. Pezone, et al., ROS in cancer therapy: the bright side of the moon, Exp. Mol. Med. 52 (2) (2020) 192–203, https://doi.org/10.1038/s12276-020-0384-2.

[35] M. Costello, T.J. Pugh, T.J. Fennell, et al., Discovery and characterization of artifactual mutations in deep coverage targeted capture sequencing data due to oxidative DNA damage during sample preparation, Nucleic Acids Res. 41 (6) (2013) e67, https://doi.org/10.1093/nar/gks1443.

[36] B. Halliwell, Why and how should we measure oxidative DNA damage in nutritional studies? How far have we come? Am. J. Clin. Nutr. 72 (5) (2000) 1082–1087, https://doi.org/10.1093/ajcn/72.5.1082.

[37] A. Valavanidis, T. Vlachogianni, C. Fiotakis, 8-hydroxy-2' -deoxyguanosine (8-OHdG): a critical biomarker of oxidative stress and carcinogenesis, J. Environ. Sci. Health C Environ. Carcinog. Ecotoxicol. Rev. 27 (2) (2009) 120–139, https://doi.org/10.1080/10590500902885684.

[38] L. Dunkenberger, K. Reiss, L. Del Valle, Comet assay for the detection of single and double-strand DNA breaks, Methods Mol. Biol. 2422 (2022) 263–269, https://doi.org/10.1007/978-1-0716-1948-3_18.

[39] A.M. Fleming, Y. Ding, C.J. Burrows, Oxidative DNA damage is epigenetic by regulating gene transcription via base excision repair, Proc. Natl. Acad. Sci. U. S. A 114 (10) (2017) 2604–2609, https://doi.org/10.1073/pnas.1619809114.

[40] P.A. Ginno, Y.W. Lim, P.L. Lott, I. Korf, F. Chédin, GC skew at the 5' and 3' ends of human genes links R-loop formation to epigenetic regulation and transcription

termination, Genome Res. 23 (10) (2013) 1590–1600, https://doi.org/10.1101/gr.158436.113.
[41] S.R. Hartono, I.F. Korf, F. Chédin, GC skew is a conserved property of unmethylated CpG island promoters across vertebrates, Nucleic Acids Res. 43 (20) (2015) 9729–9741, https://doi.org/10.1093/nar/gkv811.
[42] P. Sicińska, K. Mokra, K. Wozniak, J. Michałowicz, B. Bukowska, Genotoxic risk assessment and mechanism of DNA damage induced by phthalates and their metabolites in human peripheral blood mononuclear cells, Sci. Rep. 11 (1) (2021) 1658, https://doi.org/10.1038/s41598-020-79932-5. Published 2021 Jan 18.
[43] D.H. Phillips, V.M. Arlt, Genotoxicity: damage to DNA and its consequences, EXS 99 (2009) 87–110, https://doi.org/10.1007/978-3-7643-8336-7_4.
[44] L.A. Rowe, N. Degtyareva, P.W. Doetsch, DNA damage-induced reactive oxygen species (ROS) stress response in Saccharomyces cerevisiae, Free Radic. Biol. Med. 45 (8) (2008) 1167–1177, https://doi.org/10.1016/j.freeradbiomed.2008.07.018.
[45] A. Arora, S. Maiti, Stability and molecular recognition of quadruplexes with different loop length in the absence and presence of molecular crowding agents, J. Phys. Chem. B 113 (25) (2009 Jun 25) 8784–8792, https://doi.org/10.1021/jp809486g. PMID: 19480441.
[46] K.G. Zyner, A. Simeone, S.M. Flynn, C. Doyle, G. Marsico, S. Adhikari, G. Portella, D. Tannahill, S. Balasubramanian, G-quadruplex DNA structures in human stem cells and differentiation, Nat. Commun. 13 (1) (2022 Jan 10) 142, https://doi.org/10.1038/s41467-021-27719-1. PMID: 35013231; PMCID: PMC8748810.
[47] S. Boiteux, Properties and biological functions of the NTH and FPG proteins of escherichia coli: two DNA glycosylases that repair oxidative damage in DNA, J. Photochem. Photobiol., B 19 (2) (1993 Jul) 87–96, https://doi.org/10.1016/1011-1344(93)87101-r. PMID: 8377077.
[48] D. Gackowski, M. Starczak, E. Zarakowska, M. Modrzejewska, A. Szpila, Z. Banaszkiewicz, R. Olinski, Accurate, direct and high-throughput analyses of a broad spectrum of endogenously generated DNA base modifications with isotope-dilution two-dimensional ultraperformance liquid chromatography with tandem mass spectrometry: possible clinical implication, Anal. Chem. 88 (24) (2016 Dec 20) 12128–12136, https://doi.org/10.1021/acs.analchem.6b02900. Epub 2016 Dec 8. PMID: 28193047.